Singly versus Doubly Reduced Nickel Porphyrins for Proton Reduction: Experimental and Theoretical Evidence for a Homolytic Hydrogen-Evolution Reaction

Yongzhen Han, Huayi Fang, Huize Jing, Huiling Sun, Haitao Lei, Wenzhen Lai,* and Rui Cao*

Abstract: *A nickel(II) porphyrin **Ni-P** (P = porphyrin) bearing four meso-C_6F_5 groups to improve solubility and activity was used to explore different hydrogen-evolution-reaction (HER) mechanisms. Doubly reduced **Ni-P** ([**Ni-P**]$^{2-}$) was involved in H_2 production from acetic acid, whereas a singly reduced species ([**Ni-P**]$^-$) initiated HER with stronger trifluoroacetic acid (TFA). High activity and stability of **Ni-P** were observed in catalysis, with a remarkable i_c/i_p value of 77 with TFA at a scan rate of 100 mV s^{-1} and 20°C. Electrochemical, stopped-flow, and theoretical studies indicated that a hydride species [H-**Ni-P**] is formed by oxidative protonation of [**Ni-P**]$^-$. Subsequent rapid bimetallic homolysis to give H_2 and **Ni-P** is probably involved in the catalytic cycle. HER cycling through this one-electron-reduction and homolysis mechanism has been proposed previously but rarely validated. The present results could thus have broad implications for the design of new exquisite cycles for H_2 generation.*

Hydrogen is an ideal energy carrier to meet future energy demands.[1–5] Its generation by proton reduction is a key step in solar-to-chemical energy conversion.[6–8] Platinum is very efficient in catalyzing H_2 production, but the low natural abundance and high cost of this noble metal restrict its widespread utilization.[9,10] Progress has been made in identifying HER catalysts by the use of molecular complexes consisting of earth-abundant metals, such as Fe,[11–15] Co,[9,16–20] Ni,[21–25] and Mo.[26,27] For example, Co and Fe complexes of N-based macrocyclic ligands (e.g. diglyoxime) can operate at low overpotentials with high rates.[13,28–32] By using intramolecular

proton relays, DuBois and co-workers reported that Ni diphosphines exhibited high turnover frequencies of up to 10^5 s^{-1} at moderate overpotentials.[10] Nocera and co-workers reported that hangman groups appended to metal porphyrins could facilitate HER by mediating proton-coupled electron transfer.[22,33,34] Recently, Cu complexes have been shown to be very active for H_2 evolution by Sun and co-workers[35] and also by us.[36]

From these achievements, several factors have been identified that can facilitate H_2-evolution catalysis. However, better understanding of the HER mechanism is still necessary to provide insight for the development of efficient catalytic systems. There are five possible reaction pathways for HER mediated by metal complexes (Scheme 1). In many cases, H_2
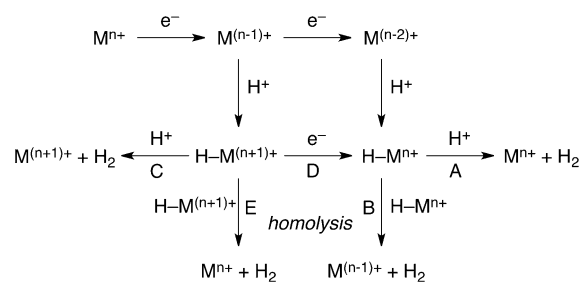
Scheme 1. Possible reaction pathways for HER mediated by metal complexes.

evolution is triggered by the 2 e$^-$ reduction of a catalyst to a M$^{(n-2)+}$ formal oxidation state, which then undergoes oxidative protonation to form a hydride intermediate H−M^{n+}.[10,16,18,30] The H−M^{n+} intermediate can either react with a proton (known as protonolysis) to release H_2 and give the starting complex M^{n+} (heterolytic route, pathway A), or react with another molecule of H−M^{n+} to give H_2 and two molecules of M$^{(n-1)+}$ (homolytic route, pathway B). In some cases, oxidative protonation of the 1 e$^-$-reduced species M$^{(n-1)+}$ occurs to form H−M$^{(n+1)+}$,[22,32,34,36] which can react with a proton to release H_2 and M$^{(n+1)+}$ (heterolytic route, pathway C) or be further reduced to form H−M^{n+} (pathway D) for subsequent H_2 generation through pathway A or B. Alternatively, the H−M$^{(n+1)+}$ intermediate can undergo bimolecular homolysis to generate H_2 and the starting complex M^{n+} (pathway E).

The 2 e$^-$ reduction/protonolysis pathways (A and D) have been well documented; however, for the 1 e$^-$ reduction/protonolysis pathway C, the H−M$^{(n+1)+}$ unit is not considered to be basic enough to drive protonolysis.[34] Unlike mono-

[*] Y. Z. Han, H. L. Sun, H. T. Lei, Prof. Dr. W. Z. Lai, Prof. Dr. R. Cao
Department of Chemistry, Renmin University of China
Beijing 100872 (China)
E-mail: wenzhenlai@ruc.edu.cn
        ruicao@ruc.edu.cn

Prof. Dr. R. Cao
School of Chemistry and Chemical Engineering
Shaanxi Normal University
Xi'an 710119 (China)

Dr. H. Y. Fang, H. Z. Jing
College of Chemistry and Molecular Engineering, Peking University
Beijing 100871 (China)

nuclear mechanisms, only a few examples of bimetallic pathways B and E have been suggested to likely be involved in HER.[28,31] For example, in a Co corrole system reported by Dey, Gross, and co-workers, pathways A and B are suspected to be possible on the basis of density functional theory (DFT) calculations.[37] By simulating the electrocatalytic cyclic voltammogram (CV) of a Fe diglyoxime catalyst, Winkler and co-workers suggested a bimetallic mechanism for H_2 evolution from a H−Fe^{III} intermediate.[13] However, they also stated that although simulation of the CV for a monometallic mechanism did not give satisfactory results, this possibility could not be ruled out. The activity comparison of a dicobaloxime and its monomeric analogue by Gray and co-workers revealed no significant enhancement, which suggests that protonolysis rather than homolysis is responsible for catalysis.[38] Therefore, a well-defined bimetallic HER mechanism has not been recognized and is of great interest and fundamental importance.

Herein, we report that **Ni-P** is a highly active and stable HER catalyst. Experimental and theoretical studies show that a bimetallic homolysis pathway is possibly involved in the catalytic HER cycle. H_2 evolution is initiated from doubly reduced species ([**Ni-P**]$^{2-}$) with acetic acid or from singly reduced species ([**Ni-P**]$^{-}$) with the stronger acid trifluoroacetic acid (TFA). The intermediate [H-**Ni-P**] from the oxidative protonation of [**Ni-P**]$^{-}$ is proposed to be able to undergo homolysis to give H_2 and the **Ni-P** starting complex with a small activation energy barrier of 3.7 kcal mol^{-1}.

We synthesized the nickel complex of 5,10,15,20-tetrakis(pentafluorophenyl)porphyrin, **Ni-P** (Figure 1). X-ray diffraction studies revealed that **Ni-P** crystallized in the tetragonal space group $I\bar{4}2d$ with the Ni atom located at the crystallographically required S_4 axis. The macrocycle of **Ni-P** is saddled rather than planar, and those pentafluorophenyl groups at *trans* positions are staggered, a conformation commonly seen in metal porphyrins.[39] The four identical N−Ni−N bond angles at 90° and Ni−N bond distances at 1.9242(14) Å suggest that the Ni atom is located perfectly at the center of the planar square defined by the four N atoms. **Ni-P** was further characterized by NMR spectroscopy and high-resolution mass spectrometry, which all confirmed the identity and purity of the bulk sample. The neutral charge of the molecule as observed in the X-ray crystal structure and its

diamagnetism as suggested by NMR spectroscopy indicated a formal d^8 Ni^{II} electronic structure.[40]

The CV of **Ni-P** was measured in acetonitrile containing 0.1 M nBu$_4$NPF$_6$. Two reversible redox couples were observed at −1.28 and −1.82 V versus ferrocene (see Figure S1 A in the Supporting Information; all potentials reported herein are vs. ferrocene). Their peak separations ΔE_p were measured to be 65 mV, thus implying two one-electron events (ΔE_p of ferrocene: 65 mV). Their peak currents displayed a linear correlation with the square root of the scan rate (see Figure S2), thus indicating two diffusion-controlled electrochemical events. The first 1 e^{-} reduction is metal-centered according to CV studies of a zinc analogue of **Ni-P** (see Figure S13) and electronic absorption spectroscopic measurements of 1 e^{-}-reduced species (see below). This assignment is also supported by studies by Savéant[41] and Nocera[22] for the 1 e^{-} reduction products of similar Ni porphyrins that were assigned as formal Ni^I species. The second reduction is ligand-centered, as found in previous studies of Ni porphyrins.[22,42,43] However, for simplicity, the formulation of [**Ni-P**]$^{-}$ and [**Ni-P**]$^{2-}$ is used hereafter for 1 e^{-}- and 2 e^{-}-reduced species, respectively.

For comparison, we also synthesized Ni complexes of 5,15-bis(pentafluorophenyl)-10,20-diphenylporphyrin and 5,10,15,20-tetrakisphenylporphyrin. We found that the replacement of *meso*-C$_6$F$_5$ by *meso*-C$_6$H$_5$ significantly decreased the solubility and caused a cathodic shift of the reduction waves. These results highlighted the significant effect of pentafluorophenyl groups in regulating the redox chemistry of Ni porphyrins. As electrocatalytic proton reduction is closely related to the reduction of catalysts, *meso* substituents with strong electron-withdrawing properties are considered to be able to cut the energy cost for generating H_2, and thus to benefit H_2 evolution, despite the fact that they might decrease the basicity of the metal center and make the metal center less reactive to protons.[28,34] This result may explain why the Co pophyrins without strong electron-withdrawing groups reported by Fukuzumi and co-workers are catalysts for O_2 reduction but not as efficient for proton reduction, as O_2 reduction is initiated by Co^{II}, whereas Co^I or Co^0 are required for proton reduction. The absence of strong electron-withdrawing substituents makes the equilibrium potentials for Co^I or Co^0 too negative to reduce protons.[44,45]

Upon the addition of acetic acid (pK_a = 22.3 in acetonitrile),[46] the second reduction peak of **Ni-P** became a catalytic wave with an onset appearing at −1.72 V (Figure 2 A). The first reduction feature was not affected much, except for the appearance of a tiny anodic wave at −1.43 V. This phenomenon has been observed in electrocatalytic HER with Ni and other metal porphyrins,[22,34] and was considered to correspond to the oxidation of protonated metal species. These results indicated that acetic acid was not strong enough to protonate the Ni center of [**Ni-P**]$^{-}$, and catalytic H_2 evolution was initiated upon 2 e^{-} reduction to [**Ni-P**]$^{2-}$. Importantly, upon the addition of TFA (pK_a = 12.7 in acetonitrile),[46] the first reduction wave exhibited pronounced catalytic activity (Figure 2 B). At low TFA concentrations, the catalytic current i_c increased linearly with the
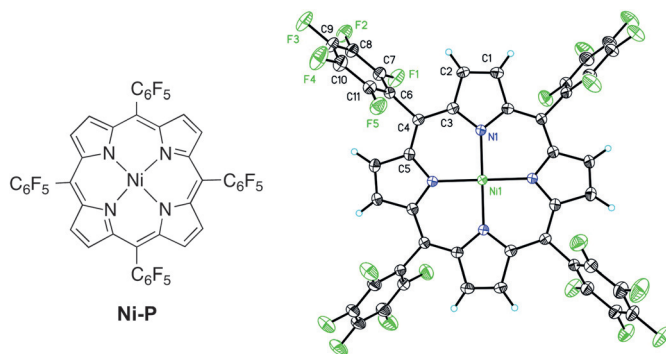

Figure 1. Molecular structure of **Ni-P** (left) and thermal-ellipsoid plot of its single-crystal X-ray structure (50% probability, right).
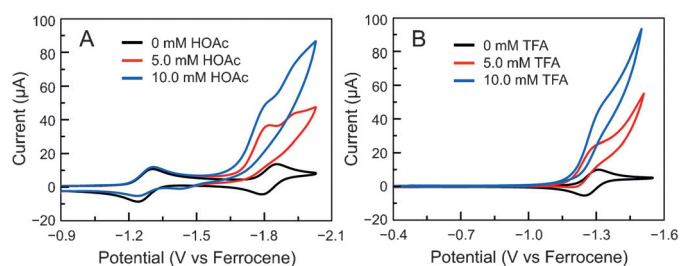
Figure 2. A) CVs of 0.50 mM **Ni-P** in acetonitrile with 0 mM (black), 5.0 mM (red), and 10.0 mM acetic acid (blue; HOAc). B) CVs of 0.50 mM **Ni-P** in acetonitrile with 0 mM (black), 5.0 mM (red), and 10.0 mM of TFA (blue). Conditions: 0.1 M Bu$_4$NPF$_6$, 0.07 cm^2 GC working electrode, 100 mVs^{-1} scan rate, 20°C.

acid concentration (see Figure S6), but reached an acid-independent region with more than 108 mM of TFA (see Figure S4). The overpotential determined at the half-wave position was approximately 420 mV with 0.1M TFA. When the acid concentration was high relative to the catalyst, i_c exhibited a linear dependence on the **Ni-P** concentration (see Figure S7). These results confirmed the molecular nature of this catalysis, and the first-order dependence of i_c on both the TFA and **Ni-P** concentrations indicated that the protonation of [**Ni-P**]$^-$ could be the rate-limiting step in H$_2$ evolution (see below). As we expected, with the Ni complex of 5,15-bis(pentafluorophenyl)-10,20-diphenylporphyrin, a later onset and smaller current were observed (see Figure S10).

Constant potential electrolysis (CPE) was performed at −1.49 V for an acetonitrile solution of 0.50 mM **Ni-P** and 0.1M TFA in a three-compartment cell. A constant current was maintained and a large amount of H$_2$ gas bubbles were observed on the surface of glassy carbon working electrode. After background correction, the amount of charge passed during electrolysis for 30 min was 0.83 C (see Figure S9), with the production of 4.2 μmol of H$_2$ as determined by gas chromatography, thus giving a Faradaic efficiency of 97% for H$_2$ generation. Therefore, the turnover number was determined to be 4.2 with an applied overpotential of 540 mV, which is comparable to reported competent HER catalysts.[10,47] The linear relationship between the charge and time suggested the stability of **Ni-P** during catalysis. After CPE for 30 min, no new species formed, as evidenced by thin-layer chromatography and UV/Vis and NMR spectroscopy, which proved that neither a demetalated porphyrin nor other porphyrin products were generated during CPE (see Figure S8). Furthermore, CPE performed at −1.82 V with a solution of 0.50 mM **Ni-P** and 10 mM acetic acid in acetonitrile generated a total of 0.24 C charge and 1.2 μmol H$_2$ in 90 min (after background correc-

tion), which gives a Faradaic efficiency of 96% and a turnover number of 1.2 for the use of acetic acid as the proton source with a 240 mV overpotential.

Complex **Ni-P** was shown to be a highly efficient HER catalyst in comparison with those reported previously from the points of view of both activity and stability. Several methods have been used previously to evaluate the performance of various HER catalysts. As one reviewer suggested, the direct comparison of the turnover numbers and turnover frequencies of different catalysts is challenging (if at all possible). Therefore, we prefer to use the i_c/i_p value (i_p is the peak current in the absence of an acid) to evaluate the catalytic efficiency of different catalyst systems under similar conditions, a ratio that has been generally reported (see Table S2 in the Supporting Information).[13,29,47–51] For **Ni-P**, the i_c/i_p value of 77 (see Figure S5) is remarkable and one of the highest among well-established competent HER catalysts. On the basis of the i_c/i_p value, a TOF of 1.2×10^3 s^{-1} can be estimated according to the generally applied method (see the Supporting Information for details).[3,4,10,25,26] On the other hand, the acid tolerance of **Ni-P** is significant: it remained unaffected in concentrated TFA solution in the dark, whereas cobaloxime and nickel diphosphine systems (the two well-known HER catalyst systems) have insufficient acid tolerance owing to the protonation of ligand-coordination sites.

Stopped-flow experiments were carried out to investigate proton reduction with **Ni-P**. The chemical reduction of **Ni-P** by sodium borohydride (NaBH$_4$) was monitored spectroscopically (Figure 3A). Upon reduction, the absorptions at 400
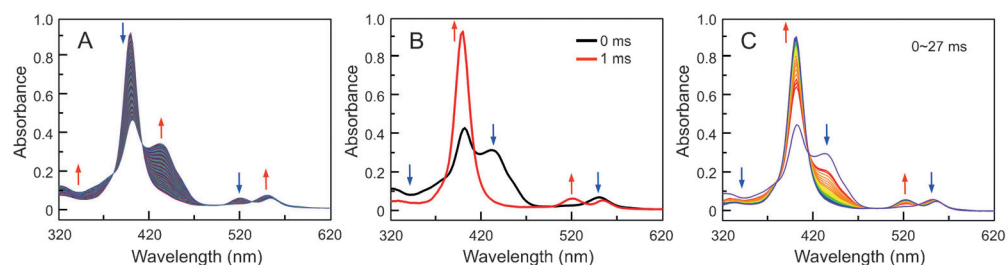

Figure 3. Stopped-flow experiments showing A) the generation of [**Ni-P**]$^-$ by NaBH$_4$, and B,C) the reaction of [**Ni-P**]$^-$ with TFA (B) and acetic acid (C).

and 520 nm decreased, whereas the absorptions at 342, 435, and 550 nm increased. The characteristic isosbestic points at 381, 413, and 534 nm indicated a clean transformation from **Ni-P** to its reduced state. These changes as well as the final electronic absorption spectrum closely resemble those observed for many other 1 e$^-$-reduced Ni porphyrins,[41–43,52] thus suggesting the formation of singly reduced species, [**Ni-P**]$^-$ (see the Supporting Information for experimental details). Upon 1 e$^-$ reduction, the Soret band at 400 nm split into two bands at 402 and 435 nm (but the overall intensity of the Soret band did not significantly decrease), and no absorption peaks developed in the 600–720 nm range (see Figure S12). These results are consistent with metal-centered reduction to give a formal Ni^I species, as established for metal porphyrins.[22,42,43,53,54]

Complete recovery of the initial UV/Vis spectrum upon the addition of TFA to a freshly prepared [**Ni-P**]⁻ solution revealed catalyst regeneration (Figure 3B). This study further confirmed the molecular nature of **Ni-P** catalysis. On the basis of this result, we propose that [**Ni-P**]⁻ first undergoes oxidative protonation with TFA to yield an [H-**Ni-P**] intermediate. Because the bimetallic homolysis of [H-**Ni-P**] yields H₂ and two equivalents of **Ni-P**, a pathway that is fully consistent with the experimental results and is found to proceed with a large thermodynamic driving force and a very small activation energy barrier (see below), we suggest that such a bimetallic homolytic route is possibly involved in the catalytic cycle. Direct protonolysis of [H-**Ni-P**] for H₂ evolution could be ruled out in this system, since this process would give H₂ and [**Ni-P**]⁺, a species not observed in our stopped-flow experiments. This phenomenon is consistent with the fact that H−M$^{(n+1)+}$ is typically not basic enough to drive protonolysis. For example, hangman Co porphyrins with three *meso*-C₆F₅ groups have been shown to electrocatalyze HER with the involvement of H−Co^{III} species.[34] However, H−Co^{III} needs to be further reduced to H−Co^{II} (pathway D in Scheme 1) for the protonolysis to yield H₂. Thermodynamic analysis of HER indicated that H−Ni^{III} (defined as [H-**Ni-P**] herein) should have a smaller driving force (by 0.41 V) to react with a proton than H−Co^{III} does (see Scheme S1 and the relevant discussion in the Supporting Information). Furthermore, thermodynamic comparison of pathways C and E revealed that HER through the bimetallic homolysis route has a larger driving force (by 0.52 V) as compared to mononuclear protonolysis. Note that NaBH₄ will be immediately consumed upon mixing with TFA. Less than 6.60×10^{-2} µmol of H₂ will be generated in this process in a 20 µL optical cell equipped with the stopped-flow instrument. Generated H₂ will have a negligible influence on the measurement, as about 6.85×10^{-2} µmol of H₂ can be dissolved in 20 µL of acetonitrile.[55]

As shown in Figure 3B, the reaction was completed in less than 1 ms, which is the shortest data-collection timescale with our stopped-flow instrument. To get more information, we replaced TFA with acetic acid to slow down the reaction. The addition of a large excess of acetic acid to the solution of [**Ni-P**]⁻ caused similar changes in the UV/Vis spectrum (Figure 3C), thus implying the regeneration of the starting catalyst. As we expected, the reaction was much slower and

took 27 ms to reach completion. This result is in accordance with CV studies, in which catalytic activity could be initiated upon the formation of [**Ni-P**]⁻ with TFA as the proton source, but catalytic H₂ evolution with acetic acid as the proton source was observed upon the formation of [**Ni-P**]²⁻ under electrochemical conditions. On the basis of these results and those from electrochemical studies, we can conclude that oxidative protonation of [**Ni-P**]⁻ is the rate-limiting step for H₂ evolution, and is followed by a fast bimetallic homolysis reaction. Therefore, the changes in the UV/Vis spectrum only showed the kinetic behavior of the protonation step in this two-step process, and the detection of the [H-**Ni-P**] intermediate is highly challenging, if it is even possible, under our experimental conditions.

To gain more insight into HER with **Ni-P**, we studied possible catalytic mechanisms by DFT calculations. The results are summarized in Figure 4. It was found that **Ni-P** has a closed-shell singlet ground state, and that the triplet state is 4.3 kcal mol⁻¹ higher in energy. The first 1 e⁻-reduced species [**Ni-P**]⁻ has two close-lying doublet states: [Ni^{I}-P]⁻
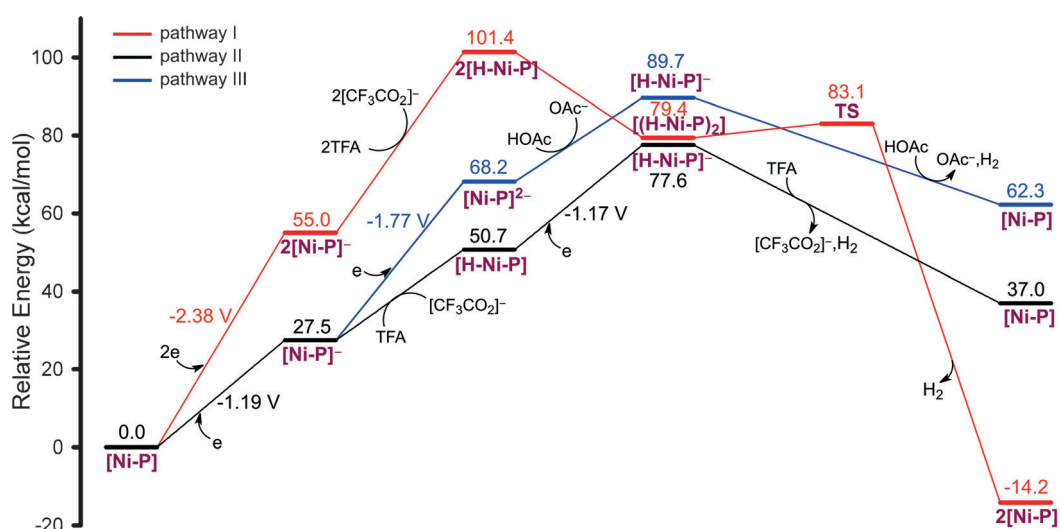

Figure 4. Energy diagram for HER catalyzed by **Ni-P**. Free-energy values are given in kcal mol⁻¹ and electrochemical potentials in volts.

and [Ni^{II}-P•⁻]⁻, generated from the reduction of Ni and porphyrin ring, respectively. Our DFT calculations show that the energetic ordering of these two states is functional-sensitive (see Table S3). Given the challenges of correctly predicting the energetic ordering in transitional-metal complexes with DFT, the doublet [Ni^{I}-P]⁻ was taken as the ground state, in agreement with the experimental results. The 2 e⁻-reduced species was found to be a Ni^{I} porphyrin radical dianion with a triplet ground state. The calculated first and second reduction potentials of **Ni-P** are −1.19 and −1.77 V, in good agreement with the experimental values (−1.28 and −1.82 V). More significantly, the calculated separation between the first and second reduction of **Ni-P** was 0.58 V, which agrees very well with the value of 0.54 V from experimental CV measurements.

Oxidative protonation of [**Ni-P**]$^-$ to generate [H-**Ni-P**] was calculated to be endothermic by 23.2 or 36.3 kcal mol^{-1} when TFA or acetic acid was used as the proton source, respectively. Although this protonation process is uphill in energy, combined stopped-flow and UV/Vis experiments indicated that proton attack on [**Ni-P**]$^-$ can occur at a high acid concentration. To explore a possible bimolecular mechanism for H$_2$ evolution, the homolytic reaction pathway of [H-**Ni-P**] was investigated. It was found that this reaction proceeds via a transition state (TS) with a very small activation energy barrier of 3.7 kcal mol^{-1} and a large exothermicity of 93.6 kcal mol^{-1} (pathway I in Figure 4). On the other hand, further 1 e$^-$ reduction of [H-**Ni-P**] gave [H-**Ni-P**]$^-$ at a calculated potential of -1.17 V, which is close to the potential of the first reduction of **Ni-P** (-1.19 V). This result suggested the possibility that [H-**Ni-P**] could be further reduced by 1 e$^-$ at the electrode during electrocatalysis. Subsequent protonolysis of [H-**Ni-P**]$^-$ to release H$_2$ and the **Ni-P** starting catalyst was calculated to be exothermic by 40.6 kcal mol^{-1} with TFA as the proton source (pathway II in Figure 4). Under conditions of chemical reduction (by NaBH$_4$), the reaction pathway via [H-**Ni-P**]$^-$ is not likely. On the basis of stopped-flow and DFT studies, we can conclude that a bimolecular homolysis mechanism for H$_2$ evolution is likely in this system, and the calculated small activation energy barrier of 3.7 kcal mol^{-1} is supportive of a fast bimetallic reaction, as established from our stopped-flow measurements.

When acetic acid was used as the proton source, the oxidative protonation of [**Ni-P**]$^-$ was found to be disfavored owing to the very large endothermicity (36.3 kcal mol^{-1}). Alternatively, oxidative protonation of [**Ni-P**]$^{2-}$ can occur to generate [H-**Ni-P**]$^-$ with a calculated endothermicity of 21.5 kcal mol^{-1}, and is followed by protonolysis to release H$_2$ and the starting catalyst (pathway III in Figure 4). Our calculations suggested that [**Ni-P**]$^{2-}$ was more favored to be involved in the electrocatalytic production of H$_2$ with acetic acid. This finding is consistent with electrochemical experiments.

In summary, our results show that **Ni-P** can electrocatalyze H$_2$ generation from acetic acid and TFA with the involvement of doubly and singly reduced active species, respectively, and is thus a valuable system for the exploration of different HER mechanisms from various acids. **Ni-P** is an extraordinary HER catalyst from the points of view of both activity and stability, with a remarkable i_c/i_p value of 77 when TFA is used as the proton source. Besides the commonly observed pathway A with acetic acid as the proton source, we propose that pathway E is likely to be involved in HER with **Ni-P** when TFA is the proton source. The bimetallic homolysis of [H-**Ni-P**], which is formed by the oxidative protonation of [**Ni-P**]$^-$, yields H$_2$ and **Ni-P**, a pathway that is fully consistent with the experimental results and is shown to proceed with a large thermodynamic driving force and a very small activation energy barrier of 3.7 kcal mol^{-1}. Our stopped-flow and DFT results showed this bimetallic reaction to be kinetically very fast. The identification of HER cycling through one-electron reduction and homolysis is highly challenging but is significant as it can provide valuable

information to enable energy input for the formation of H$_2$ to be decreased. Therefore, this study will have broad implications for the design of new exquisite cycles for H$_2$ generation.

[1] J. R. McKone, S. C. Marinescu, B. S. Brunschwig, J. R. Winkler, H. B. Gray, *Chem. Sci.* **2014**, *5*, 865–878.

[2] C. G. Morales-Guio, L. A. Stern, X. L. Hu, *Chem. Soc. Rev.* **2014**, *43*, 6555–6569.

[3] V. S. Thoi, Y. J. Sun, J. R. Long, C. J. Chang, *Chem. Soc. Rev.* **2013**, *42*, 2388–2400.

[4] M. Wang, L. Chen, L. C. Sun, *Energy Environ. Sci.* **2012**, *5*, 6763–6778.

[5] K. A. Vincent, A. Parkin, F. A. Armstrong, *Chem. Rev.* **2007**, *107*, 4366–4413.

[6] M. Grätzel, *Nature* **2001**, *414*, 338–344.

[7] T. R. Cook, D. K. Dogutan, S. Y. Reece, Y. Surendranath, T. S. Teets, D. G. Nocera, *Chem. Rev.* **2010**, *110*, 6474–6502.

[8] T. F. Jaramillo, K. P. Jørgensen, J. Bonde, J. H. Nielsen, S. Horch, I. Chorkendorff, *Science* **2007**, *317*, 100–102.

[9] J. L. Dempsey, B. S. Brunschwig, J. R. Winkler, H. B. Gray, *Acc. Chem. Res.* **2009**, *42*, 1995–2004.

[10] M. L. Helm, M. P. Stewart, R. M. Bullock, M. R. DuBois, D. L. DuBois, *Science* **2011**, *333*, 863–866.

[11] C. Tard, C. J. Pickett, *Chem. Rev.* **2009**, *109*, 2245–2274.

[12] S. Kaur-Ghumaan, L. Schwartz, R. Lomoth, M. Stein, S. Ott, *Angew. Chem. Int. Ed.* **2010**, *49*, 8033–8036; *Angew. Chem.* **2010**, *122*, 8207–8211.

[13] M. J. Rose, H. B. Gray, J. R. Winkler, *J. Am. Chem. Soc.* **2012**, *134*, 8310–8313.

[14] M. E. Carroll, B. E. Barton, T. B. Rauchfuss, P. J. Carroll, *J. Am. Chem. Soc.* **2012**, *134*, 18843–18852.

[15] C. Tard, X. M. Liu, S. K. Ibrahim, M. Bruschi, L. De Gioia, S. C. Davies, X. Yang, L. S. Wang, G. Sawers, C. J. Pickett, *Nature* **2005**, *433*, 610–613.

[16] O. Pantani, S. Naskar, R. Guillot, P. Millet, E. Anxolabéhère-Mallart, A. Aukauloo, *Angew. Chem. Int. Ed.* **2008**, *47*, 9948–9950; *Angew. Chem.* **2008**, *120*, 10096–10098.

[17] W. M. Singh, T. Baine, S. Kudo, S. L. Tian, X. A. N. Ma, H. Y. Zhou, N. J. DeYonker, T. C. Pham, J. C. Bollinger, D. L. Baker, B. Yan, C. E. Webster, X. Zhao, *Angew. Chem. Int. Ed.* **2012**, *51*, 5941–5944; *Angew. Chem.* **2012**, *124*, 6043–6046.

[18] B. Mondal, K. Sengupta, A. Rana, A. Mahammed, M. Botoshansky, S. G. Dey, Z. Gross, A. Dey, *Inorg. Chem.* **2013**, *52*, 3381–3387.

[19] H. T. Lei, A. L. Han, F. W. Li, M. N. Zhang, Y. Z. Han, P. W. Du, W. Z. Lai, R. Cao, *Phys. Chem. Chem. Phys.* **2014**, *16*, 1883–1893.

[20] Y. J. Sun, J. P. Bigi, N. A. Piro, M. L. Tang, J. R. Long, C. J. Chang, *J. Am. Chem. Soc.* **2011**, *133*, 9212–9215.

[21] M. R. DuBois, D. L. DuBois, *Chem. Soc. Rev.* **2009**, *38*, 62–72.

[22] D. K. Bediako, B. H. Solis, D. K. Dogutan, M. M. Roubelakis, A. G. Maher, C. H. Lee, M. B. Chambers, S. Hammes-Schiffer, D. G. Nocera, *Proc. Natl. Acad. Sci. USA* **2014**, *111*, 15001–15006.

[23] O. R. Luca, S. J. Konezny, J. D. Blakemore, D. M. Colosi, S. Saha, G. W. Brudvig, V. S. Batista, R. H. Crabtree, *New J. Chem.* **2012**, *36*, 1149–1152.

[24] W. A. Hoffert, J. A. S. Roberts, R. M. Bullock, M. L. Helm, *Chem. Commun.* **2013**, *49*, 7767–7769.

[25] A. M. Appel, D. H. Pool, M. O'Hagan, W. J. Shaw, J. Y. Yang, M. R. DuBois, D. L. DuBois, R. M. Bullock, *ACS Catal.* **2011**, *1*, 777–785.

[26] V. S. Thoi, H. I. Karunadasa, Y. Surendranath, J. R. Long, C. J. Chang, *Energy Environ. Sci.* **2012**, *5*, 7762–7770.

[27] H. I. Karunadasa, C. J. Chang, J. R. Long, *Nature* **2010**, *464*, 1329–1333.

[28] X. L. Hu, B. S. Brunschwig, J. C. Peters, *J. Am. Chem. Soc.* **2007**, *129*, 8988–8998.

[29] C. C. L. McCrory, C. Uyeda, J. C. Peters, *J. Am. Chem. Soc.* **2012**, *134*, 3164–3170.

[30] B. D. Stubbert, J. C. Peters, H. B. Gray, *J. Am. Chem. Soc.* **2011**, *133*, 18070–18073.

[31] P. A. Jacques, V. Artero, J. Pécaut, M. Fontecave, *Proc. Natl. Acad. Sci. USA* **2009**, *106*, 20627–20632.

[32] J. L. Dempsey, J. R. Winkler, H. B. Gray, *J. Am. Chem. Soc.* **2010**, *132*, 16774–16776.

[33] M. M. Roubelakis, D. K. Bediako, D. K. Dogutan, D. G. Nocera, *Energy Environ. Sci.* **2012**, *5*, 7737–7740.

[34] C. H. Lee, D. K. Dogutan, D. G. Nocera, *J. Am. Chem. Soc.* **2011**, *133*, 8775–8777.

[35] P. L. Zhang, M. Wang, Y. Yang, T. Y. Yao, L. C. Sun, *Angew. Chem. Int. Ed.* **2014**, *53*, 13803–13807; *Angew. Chem.* **2014**, *126*, 14023–14027.

[36] H. T. Lei, H. Y. Fang, Y. Z. Han, W. Z. Lai, X. F. Fu, R. Cao, *ACS Catal.* **2015**, *5*, 5145–5153.

[37] A. Mahammed, B. Mondal, A. Rana, A. Dey, Z. Gross, *Chem. Commun.* **2014**, *50*, 2725–2727.

[38] C. N. Valdez, J. L. Dempsey, B. S. Brunschwig, J. R. Winkler, H. B. Gray, *Proc. Natl. Acad. Sci. USA* **2012**, *109*, 15589–15593.

[39] S. Thies, C. Bornholdt, F. Köhler, F. D. Sönnichsen, C. Näther, F. Tuczek, R. Herges, *Chem. Eur. J.* **2010**, *16*, 10074–10083.

[40] Y. Z. Han, Y. Z. Wu, W. Z. Lai, R. Cao, *Inorg. Chem.* **2015**, *54*, 5604–5613.

[41] D. Lexa, M. Momenteau, J. Mispelter, J. M. Savéant, *Inorg. Chem.* **1989**, *28*, 30–35.

[42] K. M. Kadish, D. Sazou, Y. M. Liu, A. Saoiabi, M. Ferhat, R. Guilard, *Inorg. Chem.* **1988**, *27*, 1198–1204.

[43] K. M. Kadish, D. Sazou, G. B. Maiya, B. C. Han, Y. M. Liu, A. Saoiabi, M. Ferhat, R. Guilard, *Inorg. Chem.* **1989**, *28*, 2542–2547.

[44] S. Fukuzumi, K. Okamoto, Y. Tokuda, C. P. Gros, R. Guilard, *J. Am. Chem. Soc.* **2004**, *126*, 17059–17066.

[45] Y. Yamada, Y. Fukunishi, S. Yamazaki, S. Fukuzumi, *Chem. Commun.* **2010**, *46*, 7334–7336.

[46] G. A. N. Felton, R. S. Glass, D. L. Lichtenberger, D. H. Evans, *Inorg. Chem.* **2006**, *45*, 9181–9184.

[47] D. Basu, S. Mazumder, X. T. Shi, H. Baydoun, J. Niklas, O. Poluektov, H. B. Schlegel, C. N. Verani, *Angew. Chem. Int. Ed.* **2015**, *54*, 2105–2110; *Angew. Chem.* **2015**, *127*, 2133–2138.

[48] M. van der Meer, E. Glais, I. Siewert, B. Sarkar, *Angew. Chem. Int. Ed.* **2015**, *54*, 13792–13795; *Angew. Chem.* **2015**, *127*, 13997–14000.

[49] J. P. Porcher, T. Fogeron, M. Gomez-Mingot, E. Derat, L. M. Chamoreau, Y. Li, M. Fontecave, *Angew. Chem. Int. Ed.* **2015**, *54*, 14090–14093; *Angew. Chem.* **2015**, *127*, 14296–14299.

[50] E. J. Thompson, L. A. Berben, *Angew. Chem. Int. Ed.* **2015**, *54*, 11642–11646; *Angew. Chem.* **2015**, *127*, 11808–11812.

[51] U. J. Kilgore, J. A. S. Roberts, D. H. Pool, A. M. Appel, M. P. Stewart, M. R. DuBois, W. G. Dougherty, W. S. Kassel, R. M. Bullock, D. L. DuBois, *J. Am. Chem. Soc.* **2011**, *133*, 5861–5872.

[52] M. W. Renner, L. R. Furenlid, K. M. Barkigia, A. Forman, H. K. Shim, D. J. Simpson, K. M. Smith, J. Fajer, *J. Am. Chem. Soc.* **1991**, *113*, 6891–6898.

[53] G. S. Nahor, P. Neta, P. Hambright, L. R. Robinson, A. Harriman, *J. Phys. Chem.* **1990**, *94*, 6659–6663.

[54] K. M. Kadish, M. M. Franzen, B. C. Han, C. Araullo-McAdams, D. Sazou, *J. Am. Chem. Soc.* **1991**, *113*, 512–517.

[55] E. Brunner, *J. Chem. Eng. Data* **1985**, *30*, 269–273.